SuperNANO: Enabling Nanoscale Laser Anti-Counterfeiting Marking and Precision Cutting with Super-Resolution Imaging

Chen, Yiduo; Yan, Bing; Yue, Liyang; Baxter, Charlotte; Wang, Zengbo (James)

Photonics

Cyswllt i'r cyhoeddiad / Link to publication

Article

SuperNANO: Enabling Nanoscale Laser Anti-Counterfeiting Marking and Precision Cutting with Super-Resolution Imaging

Yiduo Chen [1], Bing Yan [1,2], Liyang Yue [1], Charlotte L. Jones [1] and Zengbo Wang [1,*]

1 School of Computer Science and Engineering, Bangor University, Dean Street, Bangor LL57 1UT, UK; eeu963@bangor.ac.uk (Y.C.); yan.bing@abdn.ac.uk (B.Y.); l.yue@bangor.ac.uk (L.Y.); charlotte.baxter@bangor.ac.uk (C.L.J.)

2 School of Natural and Computing Sciences, Aberdeen University, Aberdeen AB24 3FX, UK

* Correspondence: z.wang@bangor.ac.uk

Abstract: In this paper, we present a unique multi-functional super-resolution instrument, the Super-NANO system, which integrates real-time super-resolution imaging with direct laser nanofabrication capabilities. Central to the functionality of the SuperNANO system is its capacity for simultaneous nanoimaging and nanopatterning, enabling the creation of anti-counterfeiting markings and precision cutting with exceptional accuracy. The SuperNANO system, featuring a unibody superlens objective, achieves a resolution ranging from 50 to 320 nm. We showcase the instrument's versatility through its application in generating high-security anti-counterfeiting features on an aluminum film. These 'invisible' security features, which are nanoscale in dimension, can be crafted with arbitrary shapes at designated locations. Moreover, the system's precision is further evidenced by its ability to cut silver nanowires to a minimum width of 50 nm. The integrated imaging and fabricating functions of the SuperNANO make it a pivotal tool for a variety of applications, including nanotrapping, sensing, cutting, welding, drilling, signal enhancement, detection, and nanoscale laser treatment.

Keywords: superlens; nanopatterning; nanoimaging; synchronized system

1. Introduction

Laser technology has become indispensable in micro/nanopatterning due to its widespread usage. This versatile tool facilitates the precise creation of intricate structures through non-contact and maskless laser direct-writing techniques. However, a significant challenge in laser processing persists because of optical diffraction limit, particularly when aiming the production of extremely small features [1]. The minimum size of features achievable with surface patterning technologies, such as photolithography and direct laser writing, as well as the resolution of optical imaging systems, is inherently constrained by this limit. To overcome the diffraction limit, super-resolution techniques such as structured illumination microscopy, metamaterial superlenses, and microsphere superlenses have been developed [2–6]. Among these, the microsphere superlens technique is fundamental to this study. This technique is closely associated with the so-called 'photonic nanojet' effect, which helps focus light beams beyond the diffraction limit by leveraging the complex interplay of light interactions—such as reflection, refraction, and interference—occurring at the surface of micro- or nanoscale dielectric structures. This enables finer resolution in both imaging and fabrication processes [7–9]. A comprehensive review of the microsphere superlens technique, including its fundamentals and applications, can be found in our previous publication [6]. Key advancements in photonic nanojets mainly pursue two research directions: first, focusing laser beams onto the sample surface to achieve nanopatterning with sub-100 nm feature sizes, and secondly, manipulating light reflected from the sample surface, forming the foundation of super-resolution optical imaging to observe subwavelength objects and structures with resolution as fine as 45 nm [10,11].

Previous publications have demonstrated 80 nm resolution in laser nanopatterning [12] and 45–50 nm resolution in nanoimaging [10,13], alongside other notable developments [14].

The dual functional nature of the proposed system roots from the distinct particle-lens setup and super-resolution mechanism it employs. In nanopatterning experiments, it is well established that the patterning resolution is proportional to the particle size. Previous researchers have demonstrated the realization of patterning resolutions ranging from 1 μm to sub-micron levels, including sub-100 nm, using relatively small SiO_2 particle lenses [15,16]. This mechanism differs from that employed in nanoimaging. In super-resolution imaging, the microsphere superlens operates in a virtual imaging mode. It collects and transforms near-field evanescent waves, which carry high-spatial-frequency information of the object, into propagating waves that reach the far-field by forming a magnified virtual image. Here, the efficiency of evanescent-to-propagating conversion (ETPC) determines the final imaging resolution, rather than the spot size on the sample surface as in nanopatterning [17,18]. This mechanism enables the use of larger microspheres as superlenses for super-resolution imaging. At present, $BaTiO_3$ (BTG) microspheres with sizes ranging between 20 and 60 μm are widely used as dielectric superlenses [6].

Integrating both nanopatterning and nanoimaging capabilities within a single system requires design of the SuperNano objective to accommodate both working modes: focusing mode and virtual imaging mode, normally based on microsphere material, size, refractive index contrast, integration with external components, and optimization [19–22]. Additionally, the system possesses the capability to position the microsphere superlens precisely at desired locations and scan over an area, which is crucial for practical applications since a single microsphere has a limited field of view (FOV). Consequently, scanning is utilized to expand the FOV of the system for a dynamic imaging [23,24]. Various scanning schemes were used in this field, including integration with an atomic force microscope (AFM) system, encapsulation of the microsphere in a solid film, optical trapping, etc. The most recent scanning design involves bonding the microsphere superlens directly with an objective lens to create a unibody design [25,26]. In 2020, two approaches to unibody design and their applications in nanopatterning [27] and super-resolution imaging [28] were respectively published. The Plano-Convex-Microsphere (PCM) design stands out as a key innovation. It refers a compound-lens design realized by positioning a high-index microsphere onto a Plano-Convex lens and then integrating them into a conventional objective lens. However, these microsphere-based imaging and patterning systems were not integrated with each other, making real-time simultaneous nanoimaging and nanopatterning impossible. This significantly limits its applications in advanced anti-counterfeiting marking and other potential uses, such as real-time nanoscale laser processing at desired locations with nanoscale positional accuracy, biomedical applications, high-resolution diagnostic tools, and semiconductor manufacturing [29–32].

In this paper, we report a unique super-resolution instrument, SuperNANO, with dual functions of super-resolution imaging and fabrication, which realizes simultaneous label-free super-resolution imaging and direct laser nanofabrication for the first time. We present the versatility of our instrument by demonstrating its proficiency in creating anti-counterfeiting security markings on an aluminum film sample. Through real-time direct laser writing, we generate 'invisible' nano-security features (nanoscaled) with arbitrary shapes at precise locations on the sample. We demonstrate applications in two-level anti-counterfeiting marking for coveted security features, as well as nanoscissors precise directional cutting of silver nanowires with a width of 80 nm based on the synchronized nanoimaging system. In our experiments, the gap distance between the sample and lens was monitored by an auxiliary side-view microscope system which turned to be critical for achieving reliable distance control in instrumentation.

2. SuperNANO System Design

2.1. SuperNANO System Setup

Figure 1 shows the schematic of the SuperNANO system. A Thorlabs QSL103A Picosecond Microchip Laser (wavelength of 1030 nm, with a pulse duration ranging from 550 ps $\pm$ 100 ps, repetition rate of 100 kHz) is the core of the system. This laser undergoes meticulous control as it passes through a series of essential components. Initially, it encounters a precision shutter and a beam expander, both meticulously managed to ensure optimal beam quality and intensity. Subsequently, the laser enters the G3 Base galvo-scanner from Beijing JCZ Technology Co., Ltd (Beijing, China), a dynamic component capable of achieving scanning speeds of up to 5000 mm/s. This swift scanning capability facilitates precise nanopatterning on the target substrate. The setup of the SuperNANO system is partitioned into distinct left and right sections, each dedicated to specific tasks. On the left, the focus is on super-resolution fabrication, while the right segment caters to super-resolution imaging.
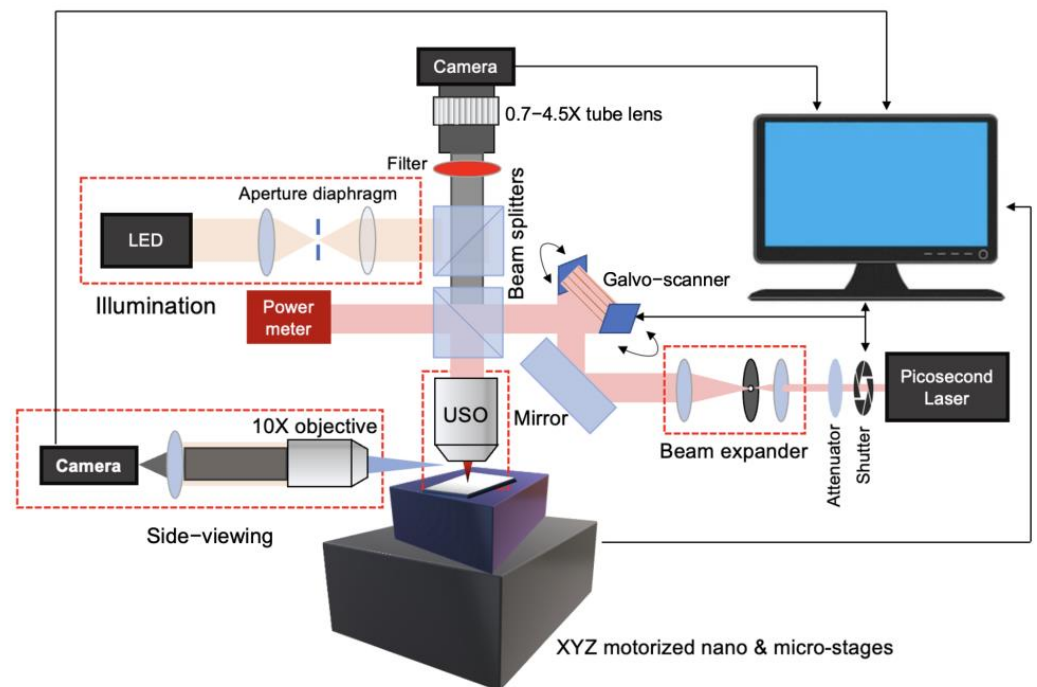

Figure 1. Schematic of the SuperNANO system setup.

These sections were combined in the middle, seamlessly sharing a common optical pathway and a pivotal component known as the unibody superlens objective (USO). This integration ensures efficient utilization of resources and facilitates seamless transitions between fabrication and imaging processes. A 50:50 beam splitter plays a role in dividing the laser beam, allocating portions for both power metering and USO operations. This division facilitates nanoimaging capabilities by directing a portion of the laser beam towards reflection and subsequent capture by a CCD camera. To further enhance precision, the system incorporates XYZ motorized nano-stage and micro-stage mechanisms, orchestrating the alignment between the USO and the substrate. Meanwhile, the illuminations are carefully curated, featuring an LED illumination and an aperture diaphragm to ensure optimal lighting conditions for nanoscale manipulation. Furthermore, the system boasts sophisticated monitoring and control functionalities, exemplified by the inclusion of a side-viewing microscope seamlessly integrated with the stage system. This combination enables real-time monitoring and precise adjustment of gap distances, further enhancing the system's capabilities in achieving unparalleled levels of precision and control in nanoscale manipulation.

2.2. Fabrication of USO

Figure 2a shows the manufacturing process of the USO lens (Figure 2b), which is based on integrating a conventional objective (with a numerical aperture of 0.65) with an 80 μm BaTiO₃ (BTG) microsphere lens in a single design, as first introduced in our previous work [33]. The two components of USO are mechanically bonded together through a transparent encapsulation layer, typically composed of ultraviolet (UV) glue or polydimethylsiloxane (PDMS). The fabrication process commences with the attachment of a microsphere onto a UV glue-coated objective (Figure 2a1), facilitated by the precise manipulation of the Z-axis of the nano-stage to position the microsphere in touch and detach from the substrate surface (see Figure 2a2,a3). Subsequently, the microsphere is secured in place through UV light curing, facilitated by the side-viewing component of the system. Challenges were encountered in accurately positioning the microsphere at the center of the USO lens during fabrication, often requiring multiple attempts to achieve the desired outcome, which affected reproducibility. To address this issue, an XY translating lens mount has been incorporated into the system (see Figure 2b). This enhancement allows for precise adjustments if the microsphere shifts, substantially increasing error tolerance during the fabrication process. Additionally, it is crucial to ensure that the thickness of the UV glue layer is less than the size of the microsphere to prevent it from becoming completely immersed. This controlled immersion not only maintains the correct focus position but is also essential for achieving optimal super-resolution performance by enabling the system to fully harness the enhancement capabilities of the microsphere lens, as demonstrated in our previous work [27].
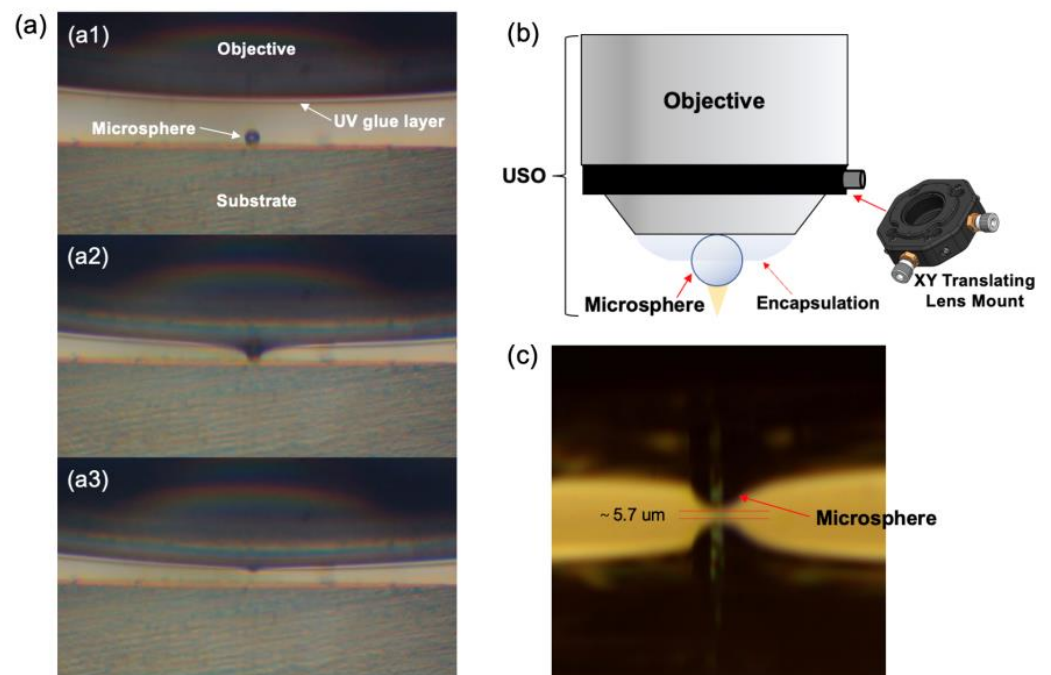
Figure 2. (**a**) Production process of USO objective made by microsphere and Plano-Convex lens: (**a1**) objective with UV glue approaching substrate, (**a2**) touching the substrate, (**a3**) detaching from the substrate. (**b**) Unibody Superlens Objective integrated with a lens mount for precise microsphere centering. (**c**) Focusing distance measurement by the side-view microscope system. The substrate acts like a mirror in the image.

In our work, the BTG microsphere used has a refractive index of 1.95, and the UV glue (NOA 60) has a refractive index of 1.52 at visible wavelengths. For super-resolution applications, a microsphere size of several to several tens of micrometers is recommended in the literature. Here, we have chosen a large-end size of 80 μm to ensure a working distance of about 5–6 μm for patterning applications. Smaller BTG microspheres would

result in a smaller working distance, making fast and reliable nanopatterning more challenging [34–36]. Furthermore, the encapsulation status of the microsphere—whether fully or partially encapsulated within the bonding layer—provides additional control over the superlens performance. Partial encapsulation, for instance, may allow for nuanced adjustments to the microsphere's position and orientation, potentially fine-tuning the focal point and enhancing the overall resolution. In short, the final focusing resolution is mainly controlled by the microsphere size, material, and encapsulation status (e.g., partial or full encapsulation).

Figure 2c depicts the measurement of the working distance of the USO objective focusing as captured by the side-view microscope system. By adjusting the Z-axis of the nano-stage, the focal length of the fabricated USO is determined to be 5.7 ± 0.03 µm. Here, the microsphere lens has a mirrored image generated by the underlying reflective substrate. This side-view imaging system not only enables accurate focal length measurements but also effectively monitors the position of the superlens, playing a crucial role in safeguarding both the lens and the sample. The USO objective is employed in both nano-imaging and laser nanofabrication processes, including nano-marking and nano-cutting as described below, to achieve enhanced resolution.

2.3. Muti-Level Laser Security Marking

Counterfeiting is a global issue and has considerable negative impacts on our society, both economically and socially. Laser marking has been used as an effective tool in anti-counterfeiting applications. Compared to ink-based marking, laser-marked patterns are difficult to rub off, making them an ideal solution for traceability and anti-counterfeiting purposes. Laser marking creates a permanent and indelible mark in various forms, including text, image, and 2D codes (QR code, Data Matrix Code, and DotCode) [28,29,37]. However, with the rapid growth of laser technology, especially fiber laser technology, the prices of conventional laser marking systems have considerably dropped in recent years, which has led to an increase in counterfeiting activities. Therefore, we need new innovations to enhance the security level of our markings, preventing counterfeiters with laser marking systems from copying or reproducing our fabrications. Here, our solution is multi-level security marking: the sample will be first marked with microscale markings, then a second level of nanoscale marking will be added by using the developed SuperNANO system. More levels of security can be realized by encoding nanoscale information in different strategies. Compared to other nanofabrication techniques such as photolithography, our technique does not involve complex processes such as spin coating, exposure, and lift off but a single step of direct laser writing. When coupled with ultrafast laser sources, the technique can be performed on almost any material surface or inside body of transparent materials [38,39].

Figure 3 shows two proposed multi-level security marking strategies. The first is the Nano inside Micro (NiM) strategy, where nanoscale markings (the letter 'S') were added to a microscale marking (the letter 'B'). The second strategy is Nano Pixel Micro (NPM), where the conventional laser marking design was first pixelized (see the pixelized 'B' in Figure 3). Each pixel is then replaced with a nano-design (the letter 'U'), either text or an image. Each pixel is laser nano-marked, and the overall fabricated image forms a micro marking image. Compared to the NiM strategy, the pixelized mark has reduced visibility but improved security.
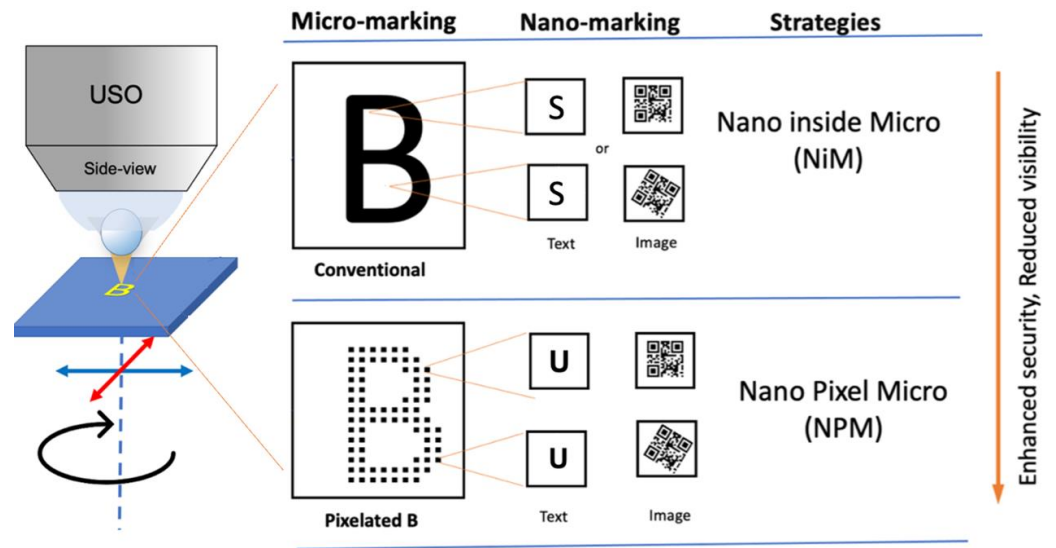
Figure 3. Strategies of multi-level laser security marking. NiM (Nano inside Micro): On top of conventional laser marking, adding designed nanopattern inside. NPM (Nano Pixel Micro): Pixelized micro-marking, replacing each pixel with designed nanopattern. The arrows indicate the movement directions of the sample stages.

3. Results and Discussion
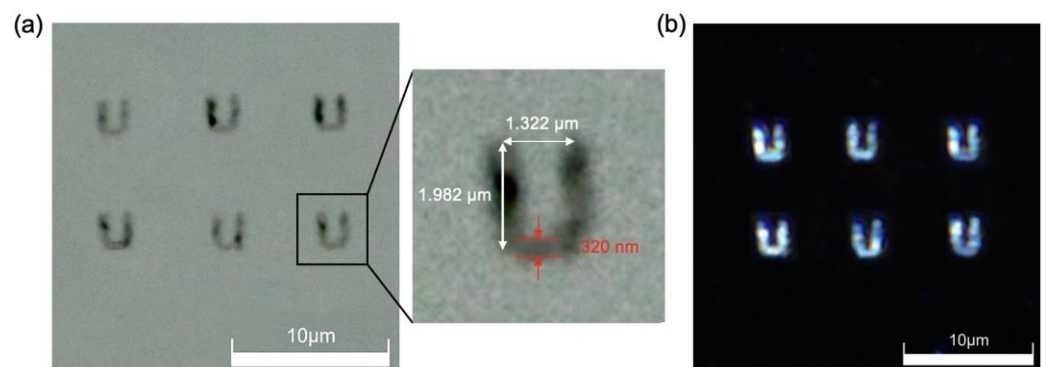
3.1. NiM Strategy Marking

Figure 4 showcases the advanced capability of the SuperNANO system in achieving nanoscale-resolution marking within microscale structures. The image displays a large 'B' letter, microscopically engraved on the surface of an aluminum sample. Zooming into the image, a smaller 'S' letter can be observed within the structure of the 'B'. In the magnified view, the dimensions of the nanoscale marking become evident, with the 'S' letter measuring approximately 330 nm in line width. This 'S' letter is etched with nanoscale precision, demonstrating the remarkable accuracy and control of the SuperNANO system in creating intricate patterns on a nanolevel. Here, the 'S' letter with nanoscale line width was marked using the USO lens described above, while the micro-sized 'B' letter was marked using conventional laser marking technology without the USO lens.
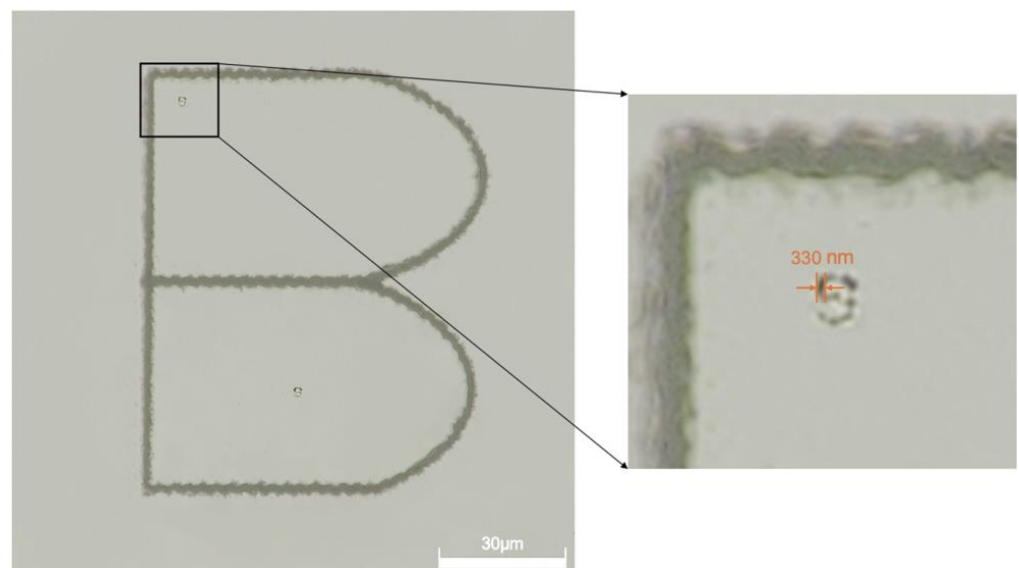
Figure 4. Microscope image of laser marked microscale 'B' letter with inside nanoscale 'S' letter.

3.2. NPM Strategy Marking

Then, we demonstrate the ability of nanoscale-resolution marking by the SuperNANO system—a microscale 'U' letter marked on the aluminum sample surface with nanoscale marking resolution, as shown in Figure 5. Each 'U' exhibits dimensions of 1.32 μm in length and 1.98 μm in width, with a marking resolution of 320 nm represented by the line width. Dark field illumination in Figure 5b emphasizes surface irregularities and variations in reflectivity by illuminating the sample from oblique angles, thereby enhancing the visibility of markings and making them stand out against the background. These irregularities are mainly caused by the small mechanical vibrations and laser energy fluctuations associated with the system. Moreover, the marking process is seamlessly integrated with the imaging system, providing real-time observation and monitoring of the fabrication process.


Figure 5. Microscope image of laser marked 'U' letters under (**a**) bright-field and (**b**) dark-field imaging modes.

Figure 6 demonstrates two examples of NPM strategy marking. In the first one, Figure 6a, the pixelated micro-sized letter 'B' is formed by nano-sized elements of 'U' with a line width of 330 nm, where BU represents Bangor University. The pixelated nanoelement offers versatility, allowing for the substitution of any desired letter form. As demonstrated in the second example in Figure 6b, the original pixel unit 'U' is replaced with 'S', forming BS representing Bangor Superlens, while maintaining a consistent line width of approximately 340 nm. Notably, the spacing between each letter, referred to as the pixel unit, is adjustable, affording precise control over the resolution of the entire pixelated letter 'B'. The spacing was set to 2 μm and 3 μm in Figures 6a and 6b, respectively. In the system, the nano-letters 'U' or 'S' are generated by a Galvo scanning beam, while the position of each letter is controlled by a micro-stage. This setup enables not only the creation of intricate pixelated structures but also offers flexibility in adjusting resolution and letter forms, making it highly adaptable to diverse nano-marking applications. However, the current fabrication process is influenced by environmental vibrations and laser energy fluctuations, which affect the uniformity of the nanostructures. Enhancing the system with advanced anti-vibration mechanisms and a more stable laser source would improve uniformity, though this would increase the overall system cost.

In the experiments mentioned above, the SuperNANO system demonstrated a 330 nm line width on an aluminum sample. However, due to challenges in achieving uniformity and stability at smaller scales on this material, we subsequently shifted our focus to nanowire cutting to better illustrate the system's capabilities. In these cutting experiments, the system achieved resolutions as fine as 50 nm, with the results visualized directly through the cutting gap sizes. These finer features, including cuts ranging from 50 nm to 280 nm—both below the demonstrated 330 nm line width—were also successfully nanoimaged using the USO lens, showcasing the SuperNANO system's ability to operate beyond the diffraction limit and achieve super-resolution imaging and fabrication.
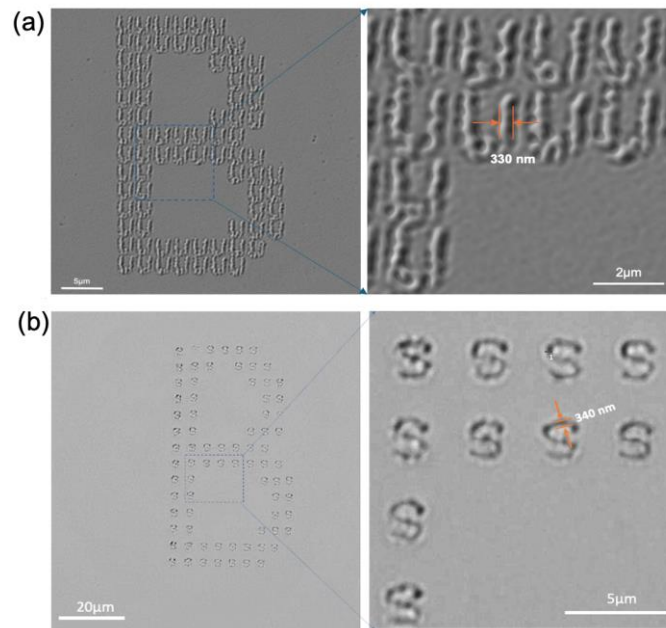
Figure 6. Microscope image of (**a**) pixelated 'B' with each pixel is marked with a nano-letter 'U', (**b**) pixelated letter 'B' with each pixel is marked with a nano-letter 'S'.
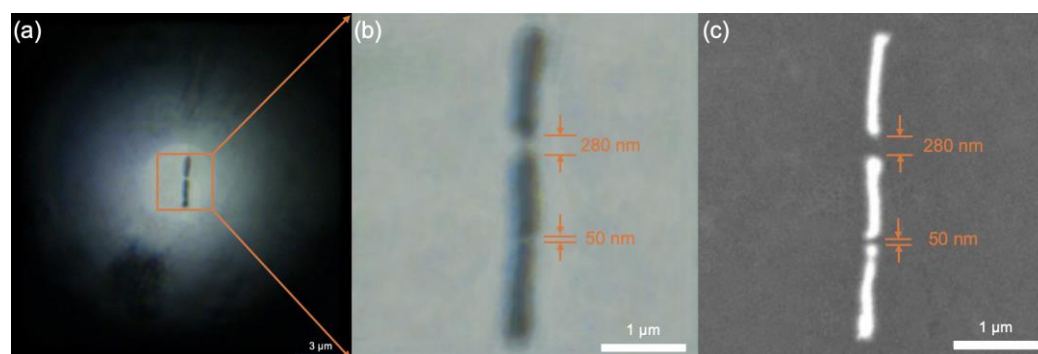
3.3. Nanowire Cutting

As explained above, to explore the resolution limit in manufacturing we performed nano-cutting experiments by the SuperNANO system on a silver nanowire (AgNW), which has many potential applications such as transparent conductive films, photovoltaics, and wearable electronics [40–42]. The AgNW was purchased from ACS MATERIAL.

As illustrated in Figure 7, the SuperNANO imaging system provides a comprehensive view of both the original and cut states of silver nanowires, showing the nanowire width around 80 nm and cutting width of approximately 440 nm. The laser fluence used is about 800 mJ/cm^2. Notably, the outline of the USO superlens is prominently visible as the circular edge shown in Figure 7, delineating the area available for imaging and laser marking. Within this white region, measuring approximately a circle with a diameter of 10 microns, lies the focal point where precise imaging and laser marking operations can be executed. This dual-functionality system seamlessly integrates imaging and marking capabilities, thereby facilitating the accurate localization of target nanowires and enabling uniform cutting at desired positions.
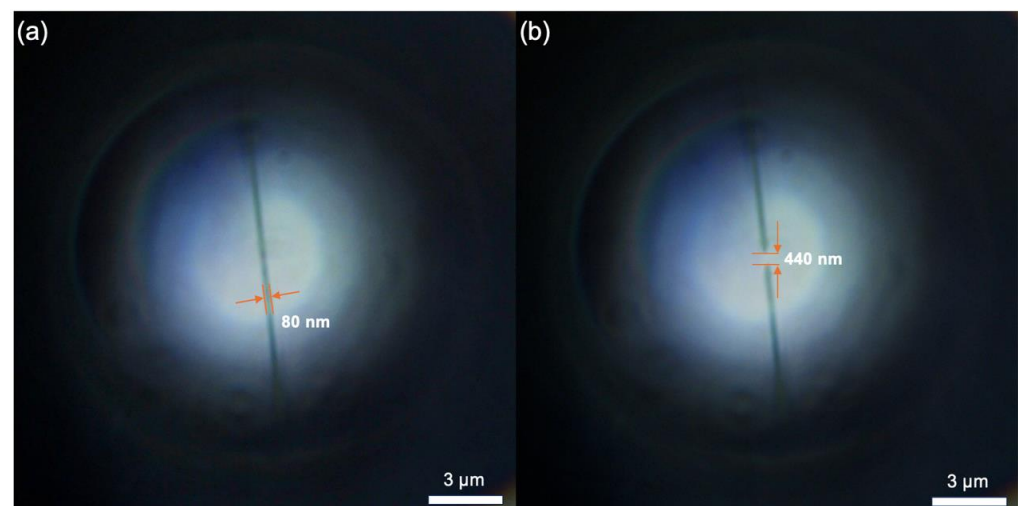
Figure 7. Example of silver nanowire cutting by SuperNANO system (**a**) before and (**b**) after cutting.

By adjusting laser fluence, we are able to control the cutting size from 50 nm to 280 nm, when laser fluence ranges from 573 mJ/cm^2 to 685 mJ/cm^2. Figure 8 shows the cutting sizes of 50 nm and 280 nm, demonstrating its cutting ability.
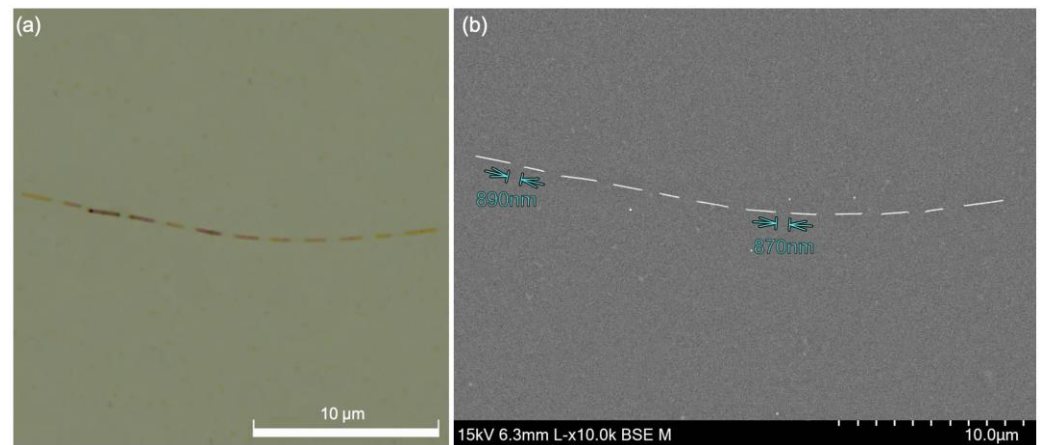

Figure 8. Silver nanowire cutting samples under (**a**) SuperNANO imaging system, (**b**) zoomed view of SuperNANO image in (**a**,**c**) SEM.

Of particular significance is the achievement of the smallest cutting width approaching less than 50 nm, underscoring a significant milestone in the capabilities of our system. This breakthrough opens up avenues for precise nanoscale manipulation with unprecedented accuracy. In subsequent stages of our research, we intend to transition to a shorter wavelength femtosecond laser, aimed at enhancing the overall stability and success rate of the cutting process. Furthermore, it is noteworthy that gaps smaller than 50 nm are only distinctly recognizable under scanning electron microscope (SEM) observation, highlighting the need for continued refinement in imaging resolution. As part of our ongoing efforts to enhance system performance, we are exploring the possibility of replacing the existing components with a higher performance TiO$_2$ superlens. This strategic upgrade holds promise for further enhancing the resolution and capabilities of the SuperNANO imaging system, thereby unlocking new possibilities in nanofabrication and nanoengineering.

Another compelling application within our research scope is the automation of nanowire ruler cutting. This process involves the utilization of a programmable micro-stage to meticulously position and cut the nanowires at specified intervals, yielding ruler-shaped nanostructures. As showcased in the results depicted in Figure 9, obtained through both microscope and SEM measurements, this automated approach offers a systematic and controlled means of fabricating nanowire-based rulers with precision and consistency. Central to the success of nanowire ruler cutting is the management of the cutting width during the cutting process. By carefully adjusting the laser energy levels, we maintain the cutting width within the range of 850–900 nm. While opting for higher energy levels may result in larger cutting widths, it is crucial for ensuring the stability and reliability of the entire automated cutting procedure.

Moving forward, our research endeavors will be dedicated to further enhancing the stability and precision of the automated cutting process. One promising avenue involves the transition to a shorter wavelength femtosecond laser, which is anticipated to offer superior stability and control over the cutting process. By harnessing the advanced capabilities of such laser technology, we aim to achieve even smaller cutting sizes in nanowire ruler cutting. In the literature, there are also reports on micro lens array (MLA)-assisted laser nanopatterning. These demonstrations are, however, based on nonlinear effects in fs laser ablation and the special materials being used. No super-resolution is associated with MLA focusing and they are not suitable for super-resolution imaging applications. Other reports on microsphere-based laser patterning techniques assisted by laser trapping or AFM positioning were also considered [43]. They are slow and complex, so they will not meet general needs for fast and reliable nanopatterning; it is also difficult to achieve dual functions, as demonstrated in our instrument. Our technique is unique in integrating real-time nanoimaging and nano-fabrication capabilities using the Unibody Superlens

Objective (USO) with a microsphere superlens. This system offers significant advantages in terms of speed and cost-effectiveness, achieving similar or better resolution compared to AFM-based or laser trapping systems while enabling rapid operation. These combined features distinguish our approach from others currently available in the literature, making it a more efficient and versatile solution for high-resolution nanopatterning and -imaging.

Figure 9. Silver nanowire ruler cutting sample under (**a**) microscope & (**b**) SEM.

In our quest for achieving finer features beyond the 50–300 nm threshold, we are exploring the adoption of either a higher performance superlens or a femtosecond laser with a shorter wavelength. One promising avenue involves the design and fabrication of a novel TiO_2 composite superlens, leveraging TiO_2 nanoparticle stacking to replace the current BTG superlens. Our recent investigations have revealed that the TiO_2 superlens consistently outperforms the BTG microsphere superlens across various metrics, including focusing spot size, imaging contrast, clarity, field of view, and imaging resolution [44]. However, the TiO_2 composite superlens may exhibit a shorter working lifespan compared to the BTG lens due to its composite nature.

4. Conclusions

In conclusion, the development of the SuperNANO instrument represents a significant advancement in nanotechnology. The demonstrated capabilities of the SuperNANO instrument extend beyond mere imaging and fabrication, encompassing applications such as two-level anti-counterfeiting marking and precise directional cutting of silver nanowires. The instrument utilizes innovative superlens technology and meticulous system design to achieve outstanding resolutions of 320 nm and 50 nm in nano-security marking and nanowire cutting, respectively. The incorporation of a nanoimaging system plays a pivotal role, enabling real-time positioning, visualization, and monitoring throughout the entire marking and fabrication process. The synergistic integration of super-resolution imaging and fabrication functionalities opens up a plethora of opportunities in various fields, including nanotrapping, -sensing, -welding, -drilling, and -signal enhancement, and -detection. Its unique combination of imaging and fabrication functions paves the way for groundbreaking advancements in a wide array of disciplines, driving innovation and pushing the boundaries of what is achievable in nanoscience and nanotechnology.

Author Contributions: Conceptualization, Z.W.; Methodology, Y.C., B.Y. and Z.W.; Validation, Y.C., B.Y., L.Y. and Z.W.; Formal analysis, Y.C. and B.Y.; Investigation, Y.C., B.Y. and C.L.J.; Writing—original draft, Y.C.; Writing—review and editing, B.Y., L.Y., C.L.J. and Z.W.; Supervision, L.Y. and Z.W.; Project administration, L.Y. and Z.W.; Funding acquisition, Z.W. All authors have read and agreed to the published version of the manuscript.

Institutional Review Board Statement: Not applicable.

Informed Consent Statement: Not applicable.

Data Availability Statement: Data are stated in the manuscript.

Conflicts of Interest: The authors declare no conflicts of interest.

References

1. Abbe, E. Beiträge zur Theorie des Mikroskops und der mikroskopischen Wahrnehmung. *Arch. Für Mikrosk. Anat.* **1873**, *9*, 413–468. [CrossRef]
2. Wang, Z.; Zhao, T.; Hao, H.; Cai, Y.; Feng, K.; Yun, X.; Liang, Y.; Wang, S.; Sun, Y.; Bianco, P.; et al. High-speed image reconstruction for optically sectioned, super-resolution structured illumination microscopy. *Adv. Photonics* **2022**, *4*, 026003. [CrossRef]
3. Wang, Z.; Zhao, T.; Cai, Y.; Zhang, J.; Hao, H.; Liang, Y.; Wang, S.; Sun, Y.; Chen, T.; Bianco, P.R.; et al. Rapid, artifact-reduced, image reconstruction for super-resolution structured illumination microscopy. *Innovation* **2023**, *4*, 100425. [CrossRef] [PubMed]
4. Chen, Z.; Taflove, A.; Backman, V. Photonic Nanojet Enhancement of Backscattering of Light by Nanoparticles: A Potential Novel Visible-Light Ultramicroscopy Technique. *Opt. Express* **2004**, *12*, 1214–1220. [CrossRef] [PubMed]
5. Lecler, S.; Takakura, Y.; Meyrueis, P. Properties of a Three-Dimensional Photonic Jet. *Opt. Lett.* **2005**, *30*, 2641–2643. [CrossRef]
6. Astratov, V.N.; Sahel, Y.B.; Eldar, Y.C.; Huang, L.; Ozcan, A.; Zheludev, N.; Zhao, J.; Burns, Z.; Liu, Z.; Narimanov, E.; et al. Roadmap on Label-Free Super-Resolution Imaging. *Laser Photonics Rev.* **2023**, *17*, 2200029. [CrossRef]
7. Wen, Y.; Yu, H.; Zhao, W.; Wang, F.; Wang, X.; Liu, L.; Li, W.J. Photonic nanojet sub-diffraction nano-fabrication with in situ super-resolution imaging. *IEEE Trans. Nanotechnol.* **2019**, *18*, 226–233. [CrossRef]
8. Wang, F.; Liu, L.; Yu, H.; Wen, Y.; Yu, P.; Liu, Z.; Wang, Y.; Li, W.J. Scanning Superlens Microscopy for Non-Invasive Large Field-of-View Visible Light Nanoscale Imaging. *Nat. Commun.* **2016**, *7*, 13748. [CrossRef]
9. Krivitsky, L.A.; Wang, J.J.; Wang, Z.; Luk'yanchuk, B. Locomotion of Microspheres for Super-Resolution Imaging. *Sci. Rep.* **2013**, *3*, 3501. [CrossRef]
10. Wang, F.; Liu, L.; Yu, P.; Liu, Z.; Yu, H.; Wang, Y.; Li, W.J. Three-Dimensional Super-Resolution Morphology by Near-Field Assisted White-Light Interferometry. *Sci. Rep.* **2016**, *6*, 24703. [CrossRef]
11. Yan, Y.; Li, L.; Feng, C.; Guo, W.; Lee, S.; Hong, M. Microsphere-Coupled Scanning Laser Confocal Nanoscope for Sub-Diffraction-Limited Imaging at 25 Nm Lateral Resolution in the Visible Spectrum. *ACS Nano* **2014**, *8*, 1809–1816. [CrossRef] [PubMed]
12. Guo, W.; Wang, Z.B.; Li, L.; Whitehead, D.J.; Luk'yanchuk, B.S.; Liu, Z. Near-Field Laser Parallel Nanofabrication of Arbitrary-Shaped Patterns. *Appl. Phys. Lett.* **2007**, *90*, 243101. [CrossRef]
13. Wang, Z.; Guo, W.; Li, L.; Luk'yanchuk, B.; Khan, A.; Liu, Z.; Chen, Z.; Hong, M. Optical Virtual Imaging at 50 Nm Lateral Resolution with a White-Light Nanoscope. *Nat. Commun.* **2011**, *2*, 218. [CrossRef] [PubMed]
14. Wang, Z.; Luk'yanchuk, B. Super-Resolution Imaging and Microscopy by Dielectric Particle-Lenses. In *Label-Free Super-Resolution Microscopy*; Astratov, V., Ed.; Springer International Publishing: Cham, Switzerland, 2019; pp. 371–406.
15. Chen, L.; Zhou, Y.; Li, Y.; Hong, M. Microsphere Enhanced Optical Imaging and Patterning: From Physics to Applications. *Appl. Phys. Rev.* **2019**, *6*, 021304. [CrossRef]
16. Khan, A.; Wang, Z.; Sheikh, M.A.; Whitehead, D.J.; Li, L. Laser Micro/Nano Patterning of Hydrophobic Surface by Contact Particle Lens Array. *Appl. Surf. Sci.* **2011**, *258*, 774–779. [CrossRef]
17. Darafsheh, A. Photonic Nanojets and Their Applications. *J. Phys. Photonics* **2021**, *3*, 022001. [CrossRef]
18. Luk'yanchuk, B.S.; Paniagua-Domínguez, R.; Minin, I.; Minin, O.; Wang, Z. Refractive Index Less than Two: Photonic Nanojets Yesterday, Today and Tomorrow [Invited]. Opt. *Mater. Express* **2017**, *7*, 1820–1847. [CrossRef]
19. Wu, G.; Hong, M. Optical Nano-Imaging via Microsphere Compound Lenses Working in Non-Contact Mode. *Opt. Express* **2021**, *29*, 23073–23082. [CrossRef]
20. Ling, J.; Li, D.; Liu, X.; Wang, X. Ultra-Long Focusing of Microsphere Lens via Wavefront Reconstruction in Microsphere. In Proceedings of the Tenth International Conference on Information Optics and Photonics, SPIE, Beijing, China, 8–11 July 2018; Volume 10964, pp. 463–468.
21. Liu, X.; Li, X.; Li, L.; Chen, W.; Luo, X. Influence of Sphere-Surface Distance and Exposure Dose on Resolution of Sphere-Lens-Array Lithography. *Opt. Express* **2015**, *23*, 30136–30142. [CrossRef]
22. Guo, M.; Ye, Y.-H.; Hou, J.; Du, B. Size-Dependent Optical Imaging Properties of High-Index Immersed Microsphere Lens. *Appl. Phys. B* **2016**, *122*, 1–7. [CrossRef]
23. Huszka, G.; Yang, H.; Gijs, M.A.M. Microsphere-Based Super-Resolution Scanning Optical Microscope. *Opt. Express* **2017**, *25*, 15079–15092. [CrossRef]
24. Yan, B.; Wang, Z.; Parker, A.L.; Lai, Y.; Thomas, P.J.; Yue, L.; Monks, J.N. Superlensing Microscope Objective Lens. *Appl. Opt.* **2017**, *56*, 3142–3147. [CrossRef]
25. Upreti, N.; Jin, G.; Rich, J.; Zhong, R.; Mai, J.; Zhao, C.; Huang, T.J. Advances in Microsphere-Based Super-Resolution Imaging. *IEEE Rev. Biomed. Eng.* **2024**, 1–16. [CrossRef] [PubMed]
26. Zhang, T.; Yu, H.; Li, P.; Wang, X.; Wang, F.; Shi, J.; Liu, Z.; Yu, P.; Yang, W.; Wang, Y.; et al. Microsphere-Based Super-Resolution Imaging for Visualized Nanomanipulation. *ACS Appl. Mater. Interfaces* **2020**, *12*, 48093–48100. [CrossRef]

27. Yan, B.; Yue, L.; Monks, J.N.; Yang, X.; Xiong, D.; Jiang, C.; Wang, Z. Superlensing Plano-Convex-Microsphere (PCM) Lens for Direct Laser Nano-Marking and Beyond. *Opt. Lett.* **2020**, *45*, 1168–1171. [CrossRef] [PubMed]

28. Yan, B.; Song, Y.; Yang, X.; Xiong, D.; Wang, Z. Unibody Microscope Objective Tipped with a Microsphere: Design, Fabrication, and Application in Subwavelength Imaging. *Appl. Opt.* **2020**, *59*, 2641–2648. [CrossRef] [PubMed]

29. Ludasi, K.; Sovány, T.; Laczkovich, O.; Hopp, B.; Smausz, T.; Regdon, G. Unique Laser Coding Technology to Fight Falsified Medicines. *Eur. J. Pharm. Sci.* **2018**, *123*, 1–9. [CrossRef]

30. Chen, Y.; Kwok, W.; Wang, Z. Enhancing Security with Superlens-Enabled Laser Direct Marking of Anti-Counterfeiting DotCode. In *Laser Science 2023*; Optica Publishing Group: Washington DC, USA; p. JM7A-34. [CrossRef]

31. Lu, Y.F.; Zhang, L.; Song, W.D.; Zheng, Y.W.; Luk'yanchuk, B.S. Laser Writing of a Subwavelength Structure on Silicon (100) Surfaces with Particle-Enhanced Optical Irradiation. *J. Exp. Theor. Phys. Lett.* **2000**, *72*, 457–459.

32. Yue, L.; Minin, O.V.; Wang, Z.; Monks, J.N.; Shalin, A.S.; Minin, I.V. Photonic Hook: A New Curved Light Beam. *Opt. Lett.* **2018**, *43*, 771–774. [CrossRef]

33. Monks, J.N.; Yan, B.; Hawkins, N.; Vollrath, F.; Wang, Z. Spider silk: Mother nature's bio-superlens. *Nano Lett.* **2016**, *16*, 5842–5845. [CrossRef]

34. Wang, J.; Barton, J.P. Actual Focal Length of a Symmetric Biconvex Microlens and Its Application in Determining the Transmitted Beam Waist Position. *Appl. Opt.* **2010**, *49*, 5828–5836. [CrossRef]

35. Li, S.; Gao, X.; Zhu, J.; Sun, Y.; Tang, T. Focusing property simulation of tapered-cladding single-mode hemispherical fiber micro-lenses. In Proceedings of the 2009 International Conference on Emerging Trends in Electronic and Photonic Devices & Systems, Varanasi, India, 22–24 December 2009; pp. 544–547.

36. Bonakdar, A.; Rezaei, M.; Brown, R.L.; Fathipour, V.; Dexheimer, E.; Jang, S.J.; Mohseni, H. Deep-UV Microsphere Projection Lithography. *Opt. Lett.* **2015**, *40*, 2537–2540. [CrossRef] [PubMed]

37. Li, X.; Yang, L.; Chang, B.; Li, T.; Li, C.; Zhang, D.; Yan, B. Simulation and Process Optimization for Laser Marking of Submillimetre Rasterizing 2D Code on Stainless Steel. *Int. J. Mod. Phys. B* **2020**, *34*, 2050266. [CrossRef]

38. Piqué, A. Chapter 1.1—Laser-Based Microadditive Manufacturing Technologies. In *Three-Dimensional Microfabrication Using Two-Photon Polymerization*; William Andrew Publishing: Norwich, NY, USA, 2020; pp. 1–23.

39. Li, Q.; Grojo, D.; Alloncle, A.-P.; Chichkov, B.; Delaporte, P. Digital Laser Micro- and Nanoprinting. *Nanophotonics* **2019**, *8*, 27–44. [CrossRef]

40. Song, Y.-J.; Chen, J.; Wu, J.-Y.; Zhang, T. Applications of Silver Nanowires on Transparent Conducting Film and Electrode of Electrochemical Capacitor. *J. Nanomater.* **2014**, *2014*, 193201. [CrossRef]

41. Kim, C.-H.; Cha, S.-H.; Kim, S.C.; Song, M.; Lee, J.; Shin, W.S.; Moon, S.-J.; Bahng, J.H.; Kotov, N.A.; Jin, S.-H. Silver Nanowire Embedded in P3HT:PCBM for High-Efficiency Hybrid Photovoltaic Device Applications. *ACS Nano* **2011**, *5*, 3319–3325. [CrossRef]

42. Huang, G.-W.; Xiao, H.-M.; Fu, S.-Y. Wearable Electronics of Silver-Nanowire/Poly(Dimethylsiloxane) Nanocomposite for Smart Clothing. *Sci. Rep.* **2015**, *5*, 13971. [CrossRef]

43. Mcleod, E.; Arnold, C.B. Subwavelength Direct-Write Nanopatterning Using Optically Trapped Microspheres. *Nat. Nanotechnol.* **2008**, *3*, 413–417. [CrossRef]

44. Dhama, R.; Yan, B.; Palego, C.; Wang, Z. Super-Resolution Imaging by Dielectric Superlenses: TiO2 Metamaterial Superlens versus BaTiO3 Superlens. *Photonics* **2021**, *8*, 222. [CrossRef]